

Interface reaction between oxide glasses and Fe–Al–Si magnetic alloy

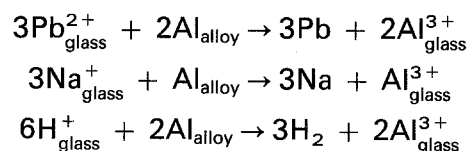
K. MATUSITA, M. SATOU*, T. KOMATSU, T. NAKAHARA

Department of Chemistry, Nagaoka University of Technology, 1603-1 Kamitomiokacho, Nagaoka, Niigata-ken 940-21, Japan

A. NITTA

Alps Electric Co. Ltd, 1-3-5 Higashi-Takami, Nagaoka, Niigata-ken 940, Japan

The interface reactions between oxide glasses and magnetic alloy, Fe–Al–Si (so-called Sendust), were analysed. The oxide glasses used were SiO₂–PbO, SiO₂–Na₂O, SiO₂–Li₂O and B₂O₃–Na₂O binary glasses. It was observed that the lattice constant of the alloy decreases and the saturation magnetic-flux density of the alloy increases on reaction with the glasses. It was found that the aluminium atoms in the alloy diffuse to the interface and dissolve into the glass melt as Al³⁺ ions, leading to the iron-rich composition of the alloy. On the other hand, Pb²⁺, Na⁺ and H⁺ ions in the molten glasses were reduced at the interface. Metallic lead particles about 20 μm in diameter were found to be dispersed in the SiO₂–PbO melt. Reduced sodium was thought to evaporate from the SiO₂–Na₂O melt, and H₂ gas bubbles were observed at the interface between B₂O₃–Na₂O melt and the alloy. These reactions were analysed based on the standard free energy diagrams of oxidation–reduction reaction, and expressed as



1. Introduction

Most devices are composed of many materials. As the chemical reactions at the interfaces affect the properties of the devices, it is important to determine the mechanism of the interface reactions thoroughly in order to develop composite devices with excellent properties. Oxide glasses have been extensively used for electromagnetic devices, such as integrated circuits and magnetic heads.

There has been little attention devoted to the chemical reactions between oxide glasses and different materials. Pask and co-workers [1–9] studied the interface reaction between metals and glasses based on the concept of wettability. Takashio [10–13] studied the interface reactions between metals and glasses from the view point of thermodynamics. Tanigawa *et al.* [14, 15] reported the reactions of Mn–Zn ferrite with lead silicate glasses and found PbO·2Fe₂O₃ is deposited during the heat treatment. Mino and Watanabe [16] studied the interface reaction between Mn–Zn ferrite and lead silicate glasses and observed that intermediate layers with many pores were formed at the interface, depending on the surface condition of the ferrite after polishing.

The interface reactions between SiO₂–PbO glass melts and various types of ferrites, such as Mn–Zn ferrite and Ni–Zn ferrite which are soft magnetic materials used for magnetic heads, were studied by Nitta *et al.* [17–20]. They reported that Mn²⁺ and Zn²⁺ ions in the ferrite dissolve into the melt as the first step, but Ni²⁺ ions had little solubility in the melt, and this dissolution process determined the whole reaction rate. Nitta *et al.* [21] also studied the effects of the third component in the glass melt on the interface reactions; the reaction between SiO₂–PbO–MO (M = Mn, Zn and Fe) ternary glasses and Mn–Zn ferrite was discussed based on the thermodynamic concept.

The Fe–Al–Si alloy, which is called Sendust, exhibits excellent soft magnetic properties and high saturation magnetization and has been developed as recording-head materials of metal-in-gap (MIG) type [22–25]. There have been only a few studies on the reactions of this alloy with the oxide glasses [25, 26].

In the present study, the mechanisms of the interface reactions between the oxide glasses and the Fe–Al–Si magnetic alloy (Sendust) were revealed using

* Present address: Research and Development Centre, Toshiba Corporation, 4-1 Ukishimacho, Kawasaki-ku, Kawasaki, Kanagawa-ken 210, Japan.

TABLE I. Glass composition, glass transition temperature, density and thermal expansion coefficient

Glass number	Batch composition (mol%)					T_g (°C)	ρ (g cm ⁻³)	λ (10 ⁷ K ⁻¹)
	SiO ₂	PbO	Na ₂ O	Li ₂ O	B ₂ O ₃			
SP64	60	40				456	5.21	75
SP55	50	50				403	6.05	95
SP46	40	60				364	6.81	113
SN21	66		34			475	2.43	149
SL21	66			34		451	2.35	110
BN21			34		66	475	2.39	106

X-ray diffraction (XRD), electron probe microanalysis (EPMA) and vibrating magnetometer.

2. Experimental procedure

The magnetic alloy, 72.3Fe–10.2Al–17.5Si (at %) was used in the present study. The glass compositions used are shown in Table 1. The glasses are denoted SP64, SP55, SP46, SN21, SL21 and BN21, for convenience. The raw materials, reagent-grade SiO₂, Pb₃O₄, Na₂CO₃, Li₂CO₃ and H₃BO₃, were placed in platinum crucibles and melted at 1400 °C for 2 h. The melts were cast on to a hot steel.

The crushed powders (about 50 µm diameter) of glasses were mixed with an equal weight of alloy powder (about 70 µm diameter) and pressed to a pellet. The pellet was heat treated under argon gas flow for 1 h at a constant temperature between 500 and 900 °C and cooled to room temperature at 2 K min⁻¹. The crystals formed in the specimen were analysed by X-ray diffraction.

In order to analyse the composition change of the interface layer, rectangular alloy specimens of 5 × 5 × 1 mm, were immersed in the glass melt in alumina crucibles at a constant temperature between 700 and 900 °C for 1 h. After heat treatment, the alloy and glass in the crucible were cooled to room temperature at a rate of 2 K min⁻¹. They were cut out from the crucible and polished into desired shapes for EPMA measurements which were carried out with a wavelength-dispersive X-ray spectroscopy (WDX). Owing to the crystallization and high viscosity, it was impossible to immerse the alloy specimens in SL21 melt.

The saturation magnetic-flux density was measured with a vibrating sample magnetometer (VSM) at an applied field of 15 kOe at room temperature, using powder samples which were crushed after heat treatment.

3. Results

Figs 1–4 show the XRD patterns of the powder mixtures of the magnetic alloy and the SP64, SN21, SL21 and BN21 glasses heat treated at various temperatures for 1 h. It is seen from Fig. 1 that metallic lead is precipitated in the mixture with SP64 glass heated at temperatures higher than 600 °C. The metallic lead was also found in the mixtures with SP55 and SP46 glasses. In the powder mixtures of the magnetic alloy and SN21 glass heated at 500 and 700 °C,

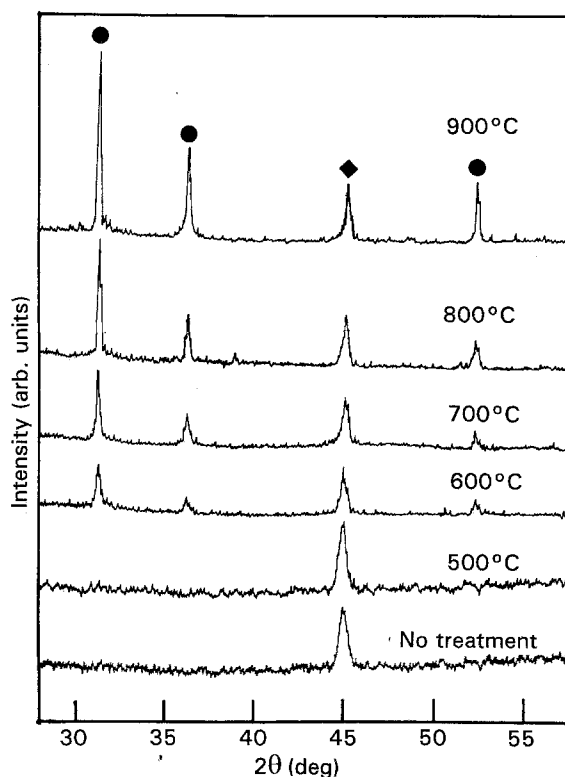


Figure 1 X-ray diffraction patterns of Fe–Al–Si alloy heated with SP64 glass at various temperatures for 1 h. (◆) Fe–Al–Si, (●) Pb.

Na₂O·2SiO₂ crystal is precipitated, as shown in Fig. 2, but in the mixture heated at 900 °C, Na₂O·Al₂O₃·2SiO₂ crystal is a main phase, indicating that aluminium atoms in the alloy were dissolved in the glass melt. In the mixtures of the alloy and SL21 glass shown in Fig. 3, Li₂O·2SiO₂ crystal is a dominant phase and small peaks of lithium aluminosilicate crystals are found in the specimen heated at 900 °C, suggesting the slow dissolution rate of aluminium in the melt. In the mixture of the alloy and BN21 glass shown in Fig. 4, metallic iron seems to be present.

Fig. 5 shows the variation of the lattice constant of the magnetic alloy with heat-treatment temperature. The specimens were the powder mixtures with various glasses and heated at each temperature for 1 h. It is seen that the lattice constant decreases with the heat-treatment temperature, suggesting that the alloy composition was changed during the heat-treatment. However, the lattice constant does not change with temperature when the alloy is heated with SL21 glass, suggesting that the alloy hardly reacts with SL21 glass.

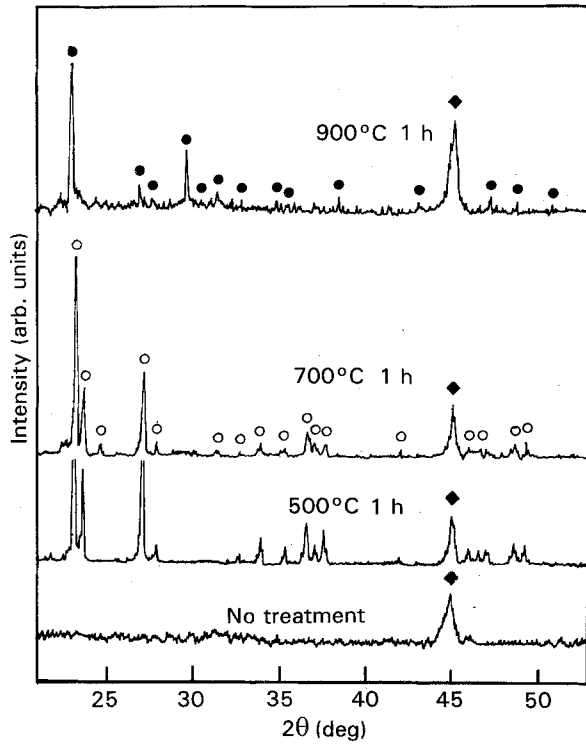


Figure 2 X-ray diffraction patterns of Fe-Al-Si alloy heated with SN21 glass at various temperatures for 1 h. (○) $\text{Na}_2\text{Si}_2\text{O}_5$, (●) Fe-Al-Si, (◆) NaAlSiO_4 .

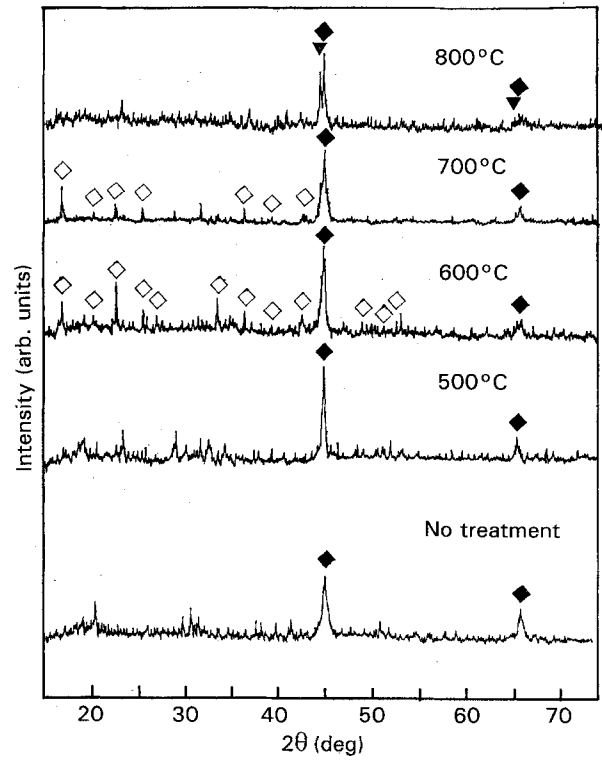


Figure 4 X-ray diffraction patterns of Fe-Al-Si alloy heated with BN21 glass at various temperatures for 1 h. (◇) $\text{Na}_2\text{B}_4\text{O}_7$, (◆) Fe-Al-Si, (▼) Fe.

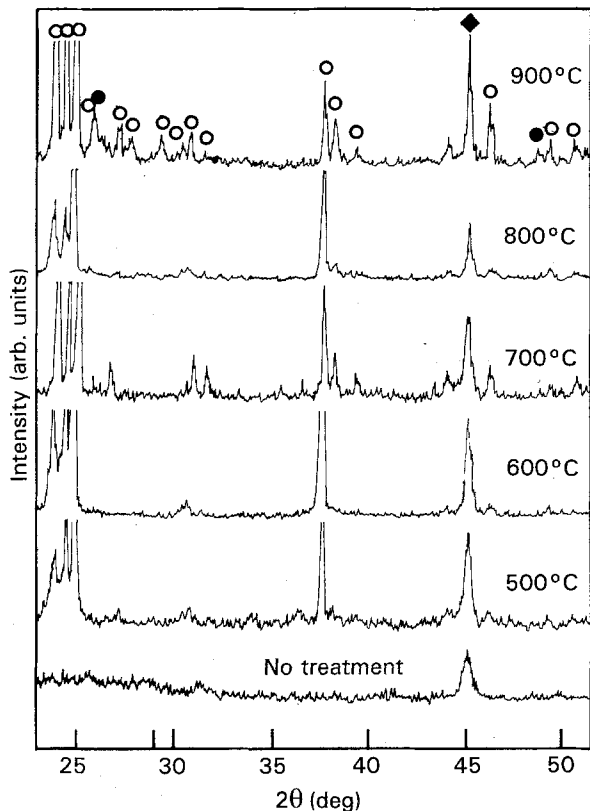


Figure 3 X-ray diffraction patterns of Fe-Al-Si alloy heated with SL21 glass at various temperatures for 1 h. (○) $\text{Li}_2\text{Si}_2\text{O}_5$, (●) $\text{Li}_x\text{Al}_x\text{Si}_{3-x}\text{O}_6$, (◆) Fe-Al-Si.

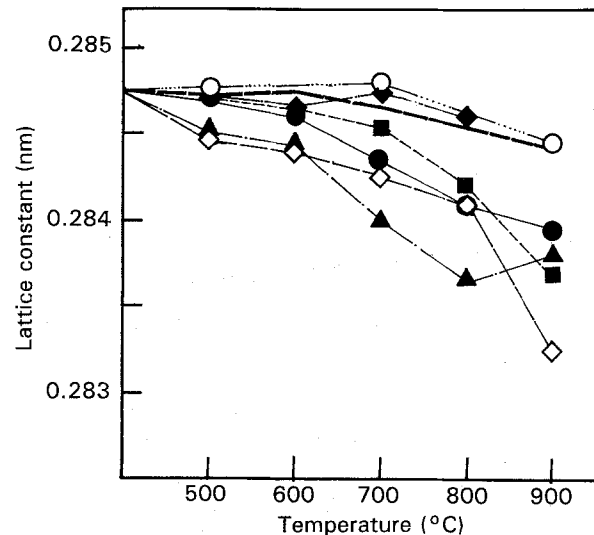


Figure 5 Lattice constant of (----) Fe-Al-Si alloy heated with glasses at various temperatures for 1 h. (■) SP64, (▲) SP55, (◇) SN21, (●) SP46, (○) SL21, (◆) BN21.

Fig. 6 shows the lines traced by WDX for the interface between the magnetic alloy and the SP64 glass heated at 750 °C for 1 h. It is clearly seen that aluminium concentrates at the interface, while other

components change smoothly through the interface. Fig. 7 shows a scanning electron micrograph of the polished cross-section of the alloy immersed in the SP64 glass and heated at 900 °C for 48 h. Particles of metallic lead, about 100–200 μm diameter, are seen in the melt close to the interface.

Fig. 8 shows a scanning electron micrograph of the interface between the alloy and BN21 glass heated at 800 °C for 1 h. It is seen that the alloy surface is corroded severely by the melt and according to EPMA, the corroded layer contains only iron.

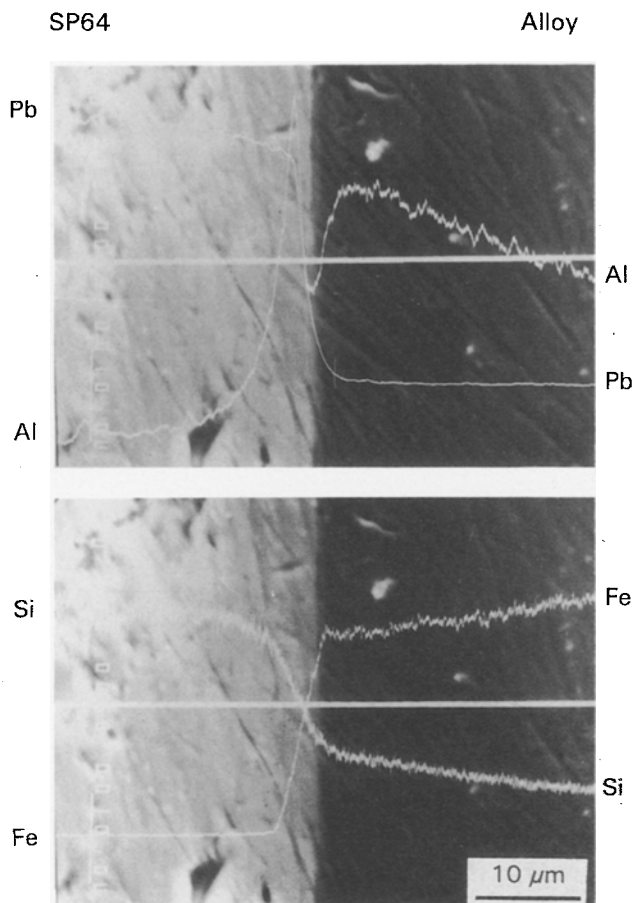


Figure 6 EPMA of the interface between Fe–Al–Si alloy and SP64 glass heated at 750 °C for 1 h.

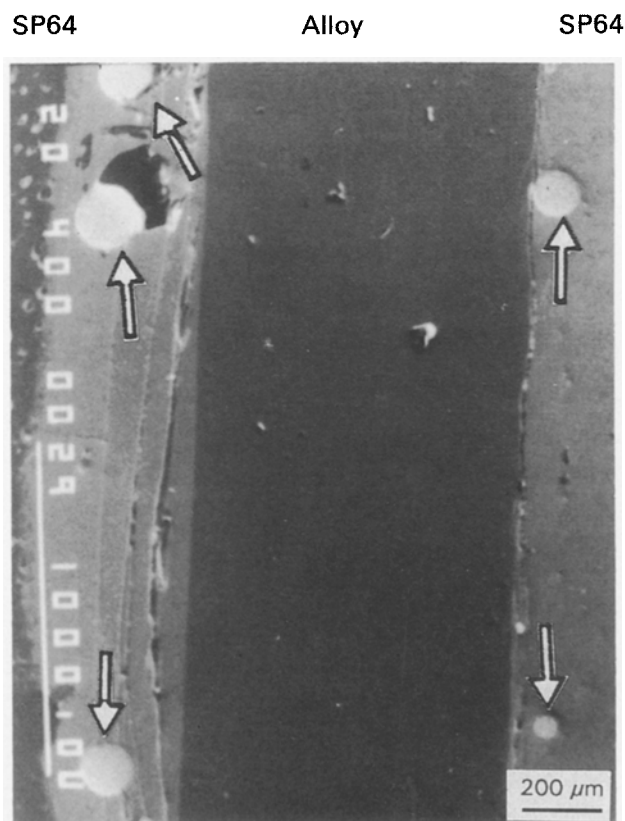


Figure 7 Scanning electron micrograph of the Fe–Al–Si alloy embedded in SP64 glass and heated at 900 °C for 48 h. Arrows indicate the lead metal.

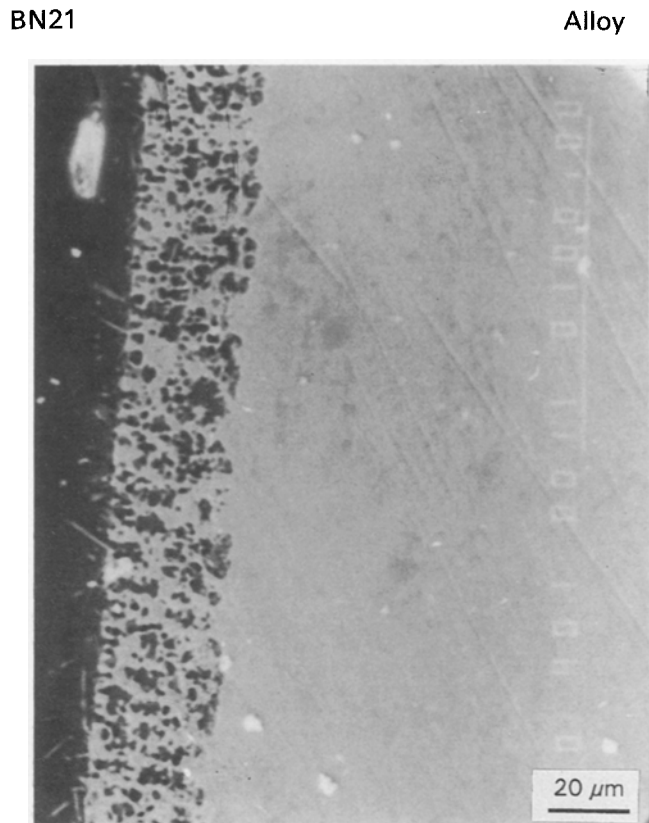


Figure 8 EPMA of the interface between Fe–Al–Si alloy and BN21 glass heated at 800 °C for 1 h.

Fig. 9a and b show the saturation magnetic flux density of the alloy powders heated with glass powders at various temperatures for 1 h. The flux density of the alloy itself without any glass powder is also shown for a comparison. It is seen, in general, that the flux density increases with the heating temperature, but the density seems to be low when heated at 600 °C.

4. Discussion

It was reported that aluminium atoms in the alloy migrate to the surface and concentrate at the surface when the alloy is heated in argon gas at high temperatures [23, 25]. In the present study, we also confirmed that Al_2O_3 was deposited on the surface when the alloy was heated at 900 °C for 1 h, even under argon gas in which the partial pressure of oxygen is very low. It has already been reported that the lattice constant of Fe–Al binary alloy increases with increasing aluminium content [27] and the lattice constant of Fe–Si binary alloy decreases with an increase in silicon content [28–30].

Fig. 10 shows the standard free energy diagrams [31] for the oxidation reaction of some elements. It is seen that aluminium atoms would be oxidized more easily than any other element in the present system except lithium, and lead would be reduced more easily than any other element.

As is seen from Fig. 1, the Pb^{2+} ions in the glass are reduced to metallic lead during heat treatment with magnetic alloy. At the same time, the aluminium atoms in the alloy diffuse to the interface and dissolve into the glass melt as Al^{3+} ions. While the metallic

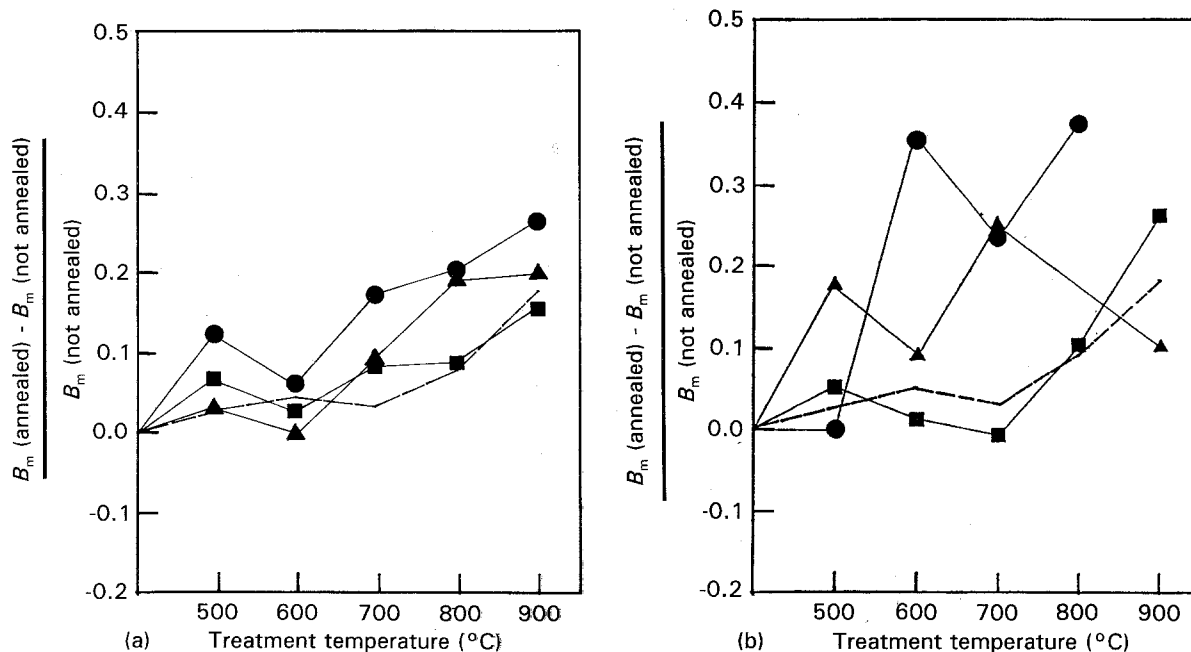


Figure 9 Saturation magnetic flux density of (---) Fe-Al-Si alloy powder heated with powders of (a) SP glasses temperatures for 1 h and (b) SN21, SL21 and BN21 glasses at various temperatures for 1 h. (a) (▲) SP64, (■) SP55, (●) SP46; (b) (▲) SL21, (●) BN21, (■) SN21.

lead particles are found to disperse in the melt, as seen from Fig. 7, the Al^{3+} ions accumulate at the interface, as shown in Fig. 6. As seen from Fig. 5, the lattice constant of the magnetic alloy powder decreases with heating temperature when heated with SP glasses, and this agrees with the dissolution of the aluminium atoms in the melt, leading to the Fe-Si-rich composition of the alloy [23, 27]. This is also consistent with the change of the saturation magnetic flux density shown in Fig. 9a. The flux density shows an abnormal decrease when heated at about 600 °C, and this may be related to the softening of the glass powder.

It is seen in Fig. 2 that $\text{Na}_2\text{O} \cdot \text{Al}_2\text{O}_3 \cdot 2\text{SiO}_2$ crystal is detected when the alloy is heated with SN21 glass, indicating the aluminium atoms in the alloy dissolve into the glass melt as Al^{3+} ions. It is thought that, according to Fig. 10, Na^+ atoms in the glass should be reduced to Na. The reduced Na is supposed to evaporate from the specimens, and the evaporation was confirmed by EPMA detection of sodium deposited on the platinum plate placed near the specimens. As seen from Fig. 5, the lattice constant of the magnetic alloy also decreases with heating temperature when heated with SN21 glass. This is also consistent with the change of the saturation magnetic-flux density shown in Fig. 9b. The flux density increases sharply at temperatures higher than 700 °C, and this may also be related to the softening of the glass powder.

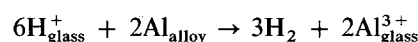
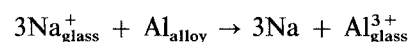
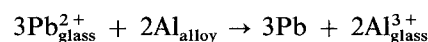
It is supposed that similar phenomena would occur for the reaction of the alloy with BN21 glass. It was observed, however, that bubbles were formed at the interface. It is known already that borate glasses generally contain a significant amount of water, nearly 0.2 mol%, when prepared by melting in air [32]. Based on the free-energy diagrams in Fig. 10, it is considered that H^+ in the glass is reduced to H_2 gas and aluminium in the alloy is dissolved in the glass as Al^{3+} ions. It is imagined that Na^+ ions may also be

reduced. It is supposed that the silicon atoms in the alloy would also dissolve into the glass melt, leading to the formation of an iron-rich phase as shown in Figs 4 and 8, and, therefore, the lattice constant of the alloy does not change with heating temperature [27–29] when heated with BN21 glass, while the saturation magnetic-flux density increases with heating temperature.

The lattice constant of the alloy is not changed by the reaction with SL21 glass. Based on Fig. 10, lithium tends to be oxidized more easily than aluminium. Therefore, it is thought that the interface reaction would not occur between the magnetic alloy and SL21 glass, or that the reaction rate is very low. In addition, it is well known that SL21 glass crystallizes very easily at low temperatures near the glass transition temperature [33, 34], and the reaction mechanism may be different from that of other glasses.

5. Conclusions

The interface reactions between oxide glasses and magnetic alloy, Fe-Al-Si (so-called Sendust) were analysed using XRD, EPMA and a vibrating sample magnetometer. It was found that aluminium atoms in the alloy diffuse to the interface and dissolve into the glass melt as Al^{3+} , and, at the same time, Pb^{2+} , Na^+ or H^+ ions in the melt are reduced. These results have been discussed based on the thermodynamics, and it was concluded that the following reactions occur at the interface between the magnetic alloy and the oxide glasses when heated at high temperatures.



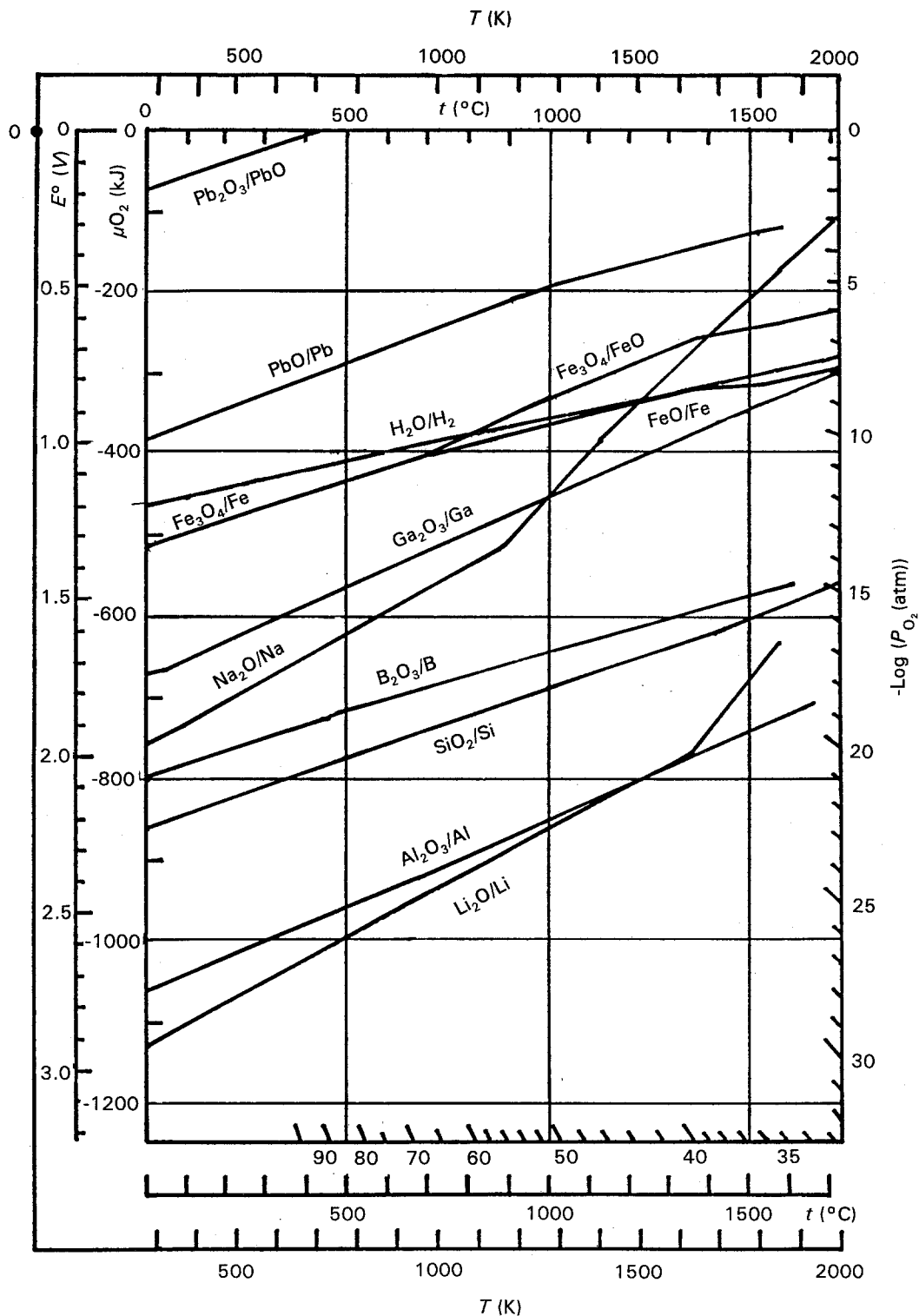


Figure 10 Standard free-energy diagrams for the formation of oxide

Acknowledgements

The present work was supported by the Japanese Ministry of Education, Science and Culture with a Grant-in-Aid for Science Research of fiscal years 1991 and 1992. The authors thank Alps Electric Company for its financial support and encouragement, and also Mr Ryuji Sato, Nagaoka University of Technology, for his experimental co-operation and fruitful discussion.

References

1. V. F. ZACKAY, D. W. MITCHELL, S. P. MITOFF and J. A. PASK, *J. Am. Ceram. Soc.* **36** (1953) 84.
2. R. M. FULRATH, S. P. MITOFF and J. A. PASK, *ibid.* **40** (1957) 269.
3. M. L. VOLP, R. M. FULRATH and J. A. PASK, *ibid.* **42** (1959) 102.
4. R. W. CLINE, R. M. FULRATH and J. A. PASK, *ibid.* **44** (1961) 423.
5. R. B. ADAMS and J. A. PASK, *ibid.* **44** (1961) 430.
6. J. A. PASK and R. M. FULRATH, *ibid.* **45** (1962) 592.
7. M. P. BOROM and J. A. PASK, *ibid.* **49** (1966) 1.
8. C. E. HOGE, J. J. BRENNAN and J. A. PASK, *ibid.* **56** (1973) 51.
9. J. J. BRENNAN and J. A. PASK, *ibid.* **56** (1973) 58.
10. H. TAKASHIO, *J. Ceram. Soc. Jpn* **82** (1974) 248.
11. *Idem*, *ibid.* **84** (1976) 383.
12. *Idem*, *ibid.* **84** (1976) 548.
13. *Idem*, *Bull. Ceram. Soc. Jpn* **15** (1980) 427.

14. H. TANIGAWA, T. UENO and K. FUKUSHIMA, *Bull. Gov. Ind. Res. Inst. Osaka* **25** (1974) 142.
15. H. TANIGAWA, T. UENO and Y. NISHIDA, *ibid.* **27** (1974) 68.
16. M. MINO and J. WATANABE, *J. Jpn. Soc. Precis. Eng.* **44** (1978) 685.
17. A. NITTA, T. MIURA, T. KOMATSU and K. MATUSITA, *J. Am. Ceram. Soc.* **72** (1989) 163.
18. A. NITTA, H. NAKAMURA, T. KOMATSU and K. MATUSITA, *ibid.* **72** (1989) 1351.
19. *Idem*, *J. Mater. Sci.* **25** (1990) 2857.
20. A. NITTA, T. KOMATSU, K. MATUSITA and A. INADA, in "Proceedings of the XV International Congress on Glass", Vol. 3b, edited by O. V. Mazurin ("Nanka", Leningrad, 1989) p. 326.
21. A. NITTA, H. NAKAMURA, T. KOMATSU and K. MATUSITA, *J. Appl. Phys.* **71** (1992) 1992.
22. T. TANAKA and M. HOMMA, *IEEE Trans. Magn.* **MAG-21** (1985) 1295.
23. M. MIYAZAKI, M. ICHIKAWA, T. KOMATSU and K. MATUSITA, *J. Appl. Phys.* **69** (1991) 1556.
24. M. MIYAZAKI, M. ICHIKAWA, T. KOMATSU, K. MATUSITA, K. NAKAJIMA and S. OKAMOTO, *ibid.* **69** (1991) 7207.
25. K. KAJIWARA, M. HAYAKAWA, Y. KUNITO, Y. IKEDA, K. HAYASHI, K. ASO and T. ISHIDA, *IEEE Trans. Magn.* **MAG-26** (1990) 2978.
26. K. MATUSITA, M. SATOU, T. KOMATSU and A. NITTA, in "Proceedings of the International Conference on Science and Technology of New Glasses" edited by S. Sakka and N. Soga (Ceramic Society of Japan, Tokyo, 1991) p. 163.
27. A. TAYLOR and R. M. JONES, *J. Phys. Chem. Solids* **6** (1958) 16.
28. M. C. FARQUHAR, *J. Iron Steel Inst.* **152** (1945) 457.
29. I. P. SELISSKII, *Z. Fiz. Khim. SSSR* **20** (1946) 597.
30. M. MIYAZAKI, M. ICHIKAWA, T. KOMATSU and K. MATUSITA, *J. Appl. Phys.* **71** (1992) 2368.
31. R. A. SWALIN, "Thermodynamics of Solids", (Wiley, New York, 1962) Fig. 7.7.
32. K. MATUSITA, T. WATANABE, K. KAMIYA and S. SAKKA, *Phys. Chem. Glasses* **21** (1980) 78.
33. P. W. McMILLAN, "Glass-Ceramics" (Academic Press, London, 1979).
34. K. MATUSITA and M. TASHIRO, *J. Non-Cryst. Solids* **11** (1973) 471.

*Received 11 June 1992
and accepted 19 March 1993*